TOWARD UNDERSTANDING FERRUGINOUS SMECTITE MG-FOR-CA INTERLAYER CATION EXCHANGE, CRYSTALLINE CA-SULFATES, AND AMORPHOUS MG-SULFATES ON MARS.

R.V. Morris[1], D.T. Vaniman[2], J.V. Clark[3], E.B. Rampe[1], D.W. Ming[1], C.N. Achilles[4], D.P. Archer[3]. [1]NASA JSC, Houston, TX, [2]PSI, Tucson, AZ, [3]Jacobs, NASA JSC, Houston, TX, [4]NASA GSFC, Greenbelt, MD.

Introduction. Crystalline Ca-sulfate minerals (gypsum $CaSO_4 \cdot 2H_2O$; bassanite $CaSO_4 \cdot 0.5H_2O$; and anhydrite $CaSO_4$) were detected in most X-ray diffraction patterns acquired to date by the CheMin transmission XRD instrument [1] onboard the Mars Science Laboratory (MSL) rover *Curiosity* during its ongoing mission at Gale crater [e.g., 2-10]. Relative proportions of Ca-sulfate minerals vary from sample-to-sample and, in some case, vary during multi-sol CheMin analyses in response to different environmental conditions in situ and within the CheMin instrument [11]. Chemical associations of Ca and S are prevalent at Gale crater, particularly in Ca-sulfate-rich veins that penetrate local sedimentary rock [e.g., 12-14]. No other crystalline monocation sulfates or their hydrated equivalents (e.g., $MgSO_4 \cdot nH_2O$) have yet been detected by CheMin though chemical associations (e.g., Mg and S) are present [e.g., 12-14].

No detection of crystalline monocation sulfates by CheMin, excepting Ca-sulfates, implies other monocation sulfates (e.g., $MgSO_4$, $MnSO_4$, $FeSO_4$, and $Fe_2(SO_4)_3$ and hydrated equivalents) are present below CheMin detection limits, are XRD amorphous [e.g., 15-18], or were not sampled. We advance here a pathway for precipitation of crystalline Ca-sulfates and amorphous Mg-sulfate based on experimental evidence for replacement of Ca interlayer cations in smectite SWa-1 by Mg sourced from Mg sulfate solutions.

Samples and Methods. Clay Mineral Society smectite SWa-1 was purified as a <0.5 µm size fraction by grinding, sonic probe disaggregation, Stokes-Law settling in deionized water, and centrifuging and washing multiple times with deionized water. Air dried purified powder is referred to here as SWa1_ORIG. A 1.0 g portion was combined with 10 g of Ca-free, 0.05 M $MgSO_4$ reagent solution, and resulting the suspension was agitated on a shaker arm at ~25 °C for 21 d. After agitation, a split was air dried (SWa1_EVAP), and remaining sample subjected to two centrifuge (8000 rpm for ~40 min), decant, and wash cycles with deionized water (no intervening drying) before air-drying (SWa1_WASH). Samples were analyzed by XRD (Siemens D500 at LANL and CheMin-4 (CM4) at JSC), VNIR reflectance spectroscopy (ASD FieldSpec3 at JSC) in air or N_2 purged glove box (25°C; RH~0.4%), thermogravametric (TG) analysis (Netzsch STA F1 Jupiter coupled to Pfeiffer QMS at JSC; He/1000mbar/3sccm), and XRF (Rigaku ZSX at LANL). VNIR peak positions were determined from continuum-removed spectra.

Results and Discussion. The SWa1_ORIG XRD pattern (Fig. 1) is typical for ferric dioctahedral smectites with 001 reflections at 15.2 Å in air and 13.6 Å in dry N_2 and at 02L reflections at 4.50 Å for both atmospheres. The smectite pattern is invariant across all three samples, and gypsum peaks are present only for SWa1_EVAP.

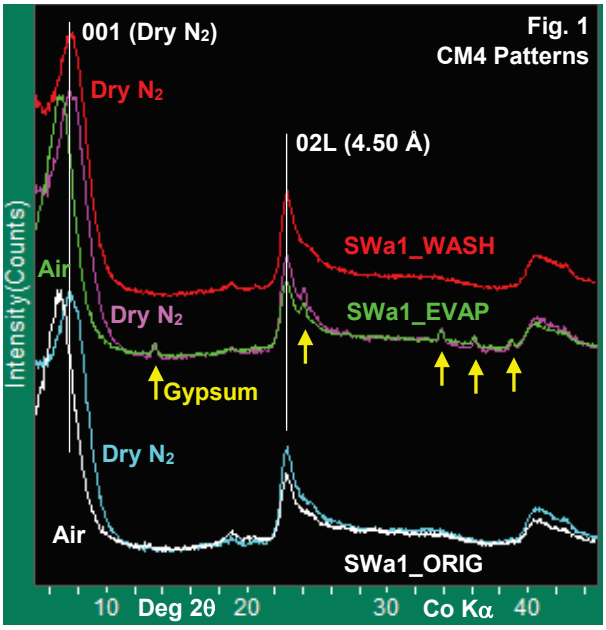

The XRD patterns are interpreted as follows: (1) Ca is initially present only as an interlayer cation (ORIG); (2) Mg partially replaced Ca as the smectite interlayer cation, and gypsum precipitated from the suspartially pension during air drying (EVAP); and (3) gypsum and (if present) XRD amorphous Mg-sulfate were removed by dissolution during washing, leaving only smectite with enhanced Mg/Ca ratio (WASH). Crystalline Mg-sulfate phases were not detected in EVAP. Confirming XRD interpretations, XRF analyses show Ca concentrations decrease (0.33 to 0.18 cations/22O) and Mg concentratins increase (0.40 to 0.57 cations/22O) in WASH relative to ORIG. We cannot exclude, with XRD data alone, either low concentrations of amorphous Mg-sulfate in EVAP or minor incorporation Mg into semectite octahedral sites. Both are unsupported by other data as discussed next.

XRD patterns (dry N_2 instrumment purge) for amorphous Mg-sulfate from solid-state desiccation of epsom salts (dry N_2 glove-box purge) are charactherized by two broad humps centered near 18 and 31 deg. 2θ (Fig. 2a), similar to amorphous Mg-sulfates from vacuum desiccation and cryo-precipitation [e.g., 15-19]. TG data (Fig. 2b) for one sample represent it as a dihydrate (similar to [15,16]) with dehydration and

desulfurization near 200°C and 1100°C, respectively.

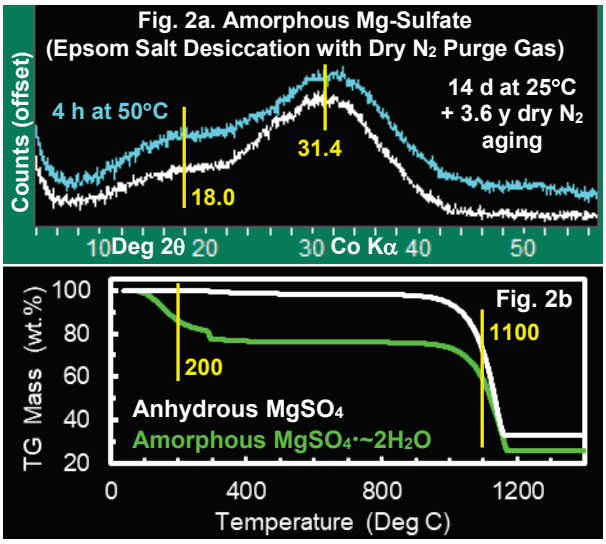

VNIR spectra for amorphous Mg-sulfates from solid-state desiccation of epsom salt (Fig 3a; spectra acquired under desiccating conditions) are characterized entirely by OH and HOH vibrational features. The spectra are distinct from kieserite (crystalline $MgSO_4.H_2O$) with its 2.10 µm spectral feature and similar to other crystalline and hydrated Mg-sulfates (esp. starkeyite and pentahydrite [e.g., 20]), terrestial materials including smectites that are associated with the H_2O molecule, and martian surface spectra typically interpreted as representing "polyhyrdrated sulfate" [21].

VNIR spectra for untreated (ORIG) and treated (EVAP and WASH) (Fig. 3b; spectra acquired in air) are characterized by Fe^{3+} electronic spectral features near 0.42, 0.66, and 0.97 µm and OH/H_2O vibrational features near 1.4 and 1.9 µm and between ~2.2 and ~2.5 µm. The Fe^{3+} and OH/H_2O 1.4 and 1.9 µm features are attributed to SWa-1 with interlayer sites occupied by Ca (ORIG) and Mg (EVAP and WASH) with possible contributions from amorphous Mg-Sulfate to EVAP with weakest OH/H_2O features (0.98 and 1.17 µm) being masked by more intense smectite Fe^{3+} features.

Smectite cation-hydroxyl vibrational spectral features occur between ~2.1 and ~2.5 µm, and their positions and intensities are equivalent for our three samples (Fig. 3b; inset). Assignments are (Fe,Fe)-OH (2.29 µm), (Al,Fe)-OH (2.24 µm), and (Al,Al)-OH (shoulder below ~2.24 µm). A 2.31 µm spectral feature for (Mg,Mg)-OH was not detected for EVAP and WASH, confirming XRD data that Mg is present as an interlayer and not an octahedral cation. If amorphous Mg-SO_4 is not present in EVAP, the smectite incorporated all aqueous Mg as interlayer cations.

Applications to Mars. (1) Formation pathways for locally-sourced crystalline Ca-sulfate minerals and concomitant Mg-enriched smectite include Mg for Ca exchange of smectite interlayer cations from percolating Mg-bearing solutions and local precipitation of Ca-sulfates. (2) Interlayer cation exchange and aqueous Ca transport can result in sulfate diagenetic features with Ca in-part to wholly sourced from smectite interlayer Ca. (3) Orbital spectral signatures of martian optical surfaces interpreted as consistent with Mg polyhydrated sulfate [21] are consistent the signature of amorphous Mg-sulfate. (4) This study corrobarates results of [22] showing that smectite, zeolites, and palagonite can all produce gypsum from pure Mg-sulfate solution by cation exchange, but of these smectite is most effective.

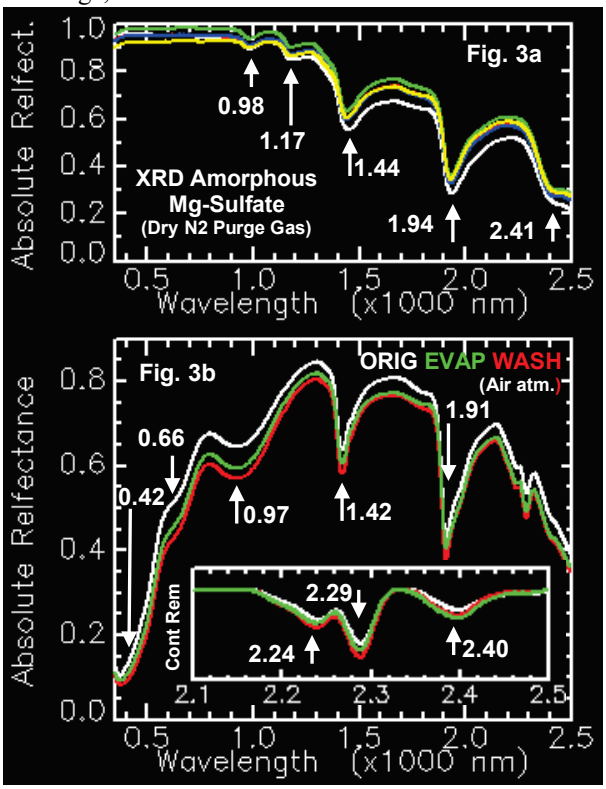

References: [1] Blake *et al.* (2012) *Space Sci. Rev.*, doi: 10.1007/s11214-012-9905-1. [2] Bish *et al.* (2013) *Science 341*, doi:10.1007/s11214-012-9905-1. [3] Vaniman *et al.* (2014) *Science 343*, doi:10.1126/science.1243480. [4] Morris *et al.* (2016) *PNAS 113*, 7071. [5] Achilles *et al.* (2017) *JGRE 122*, doi:10.1002/2017je005262. [6] Rampe *et al.* (2017) *EPSL 471*, 172. [7] Yen *et al.* (2017) *EPSL 471*, 186. [8] Morrison *et al.* (2018) *AmMin*, doi:10.2138/am-2018-6124. [9] Rampe *et al.* (2020) *JGRE 125*, doi:/10.1029/2019JE006306. [10] Achilles *et al.* (2020) *JGRE 125*, doi: /10.1029/2019JE006295. [11] Vaniman *et al.* (2018) *AmMin*, doi.org/10.2138/am-2018-6346. [12] Nachon *et al.* (2014) *JGRE 119*, 1991. [13] Nachon *et al.* (2017) *Icarus 281*, 121. [14] Berger *et al.* (2020) *JGRE 125*, doi:10.1029/2020JE006536. [15] Vaniman *et al.* (2004) *Science 431*, 665. [16] Wang *et al.*, (2006) *GCA 70*, 6118. [17] Chipera and Vaniman (2007) *GCA 71*, 241. [18] Vaniman *et al.* (2011) *LPSC42*, 2276. [19] Morris *et al.* (2015) *LPSC46*, 2434. [20] Crowley (1991) *JGR 96*, 16231. [21] Sheppard *et al.* (2021), *JGRE accepted,* doi:10.1029/2020JE006372. [22] Vaniman and Chipera (2006) *AmMin* doi:10.2138/am.2006.2092 91, 1628.